Concept for polychromatic laser guide stars: one-photon excitation of the 4P3/2 level of a sodium atom

J. P. Pique, Ioana Cristina Moldovan, Vincent Fesquet

HAL Id: hal-01118423
https://hal.science/hal-01118423

A new concept for polychromatic laser guide stars : one photon excitation of 4P$_{3/2}$ level of sodium atom

J.P. Pique, I. Moldovan and V. Fesquet

Laboratoire de Spectrométrie Physique, Université Joseph Fourier, UMR 5588 CNRS-

Grenoble I, B.P. 87, 38402 saint Martin d'Hères, FRANCE

Abstract

The correction of the atmospheric tip-tilt using a polychromatic laser guide star (PLGS) is the only solution currently suggested to run the adaptive optics of ground telescopes over 100% of the sky. The difficulty is to create a sufficiently intense UV chromatic component of the PLGS. We show that, if one uses a gravity centre technique, the returned flux of photons at 330nm must lie between 2×10^5 photons/s/m^2 and 1.3×10^6 photons/s/m^2. This paper describes a model which is validated on experimental results on the sky at the observatory of Keck, the LLNL and Pierrelatte. We give the results of this model for the solution already suggested which consists in exciting the 4D$_{5/2}$ level of mesospheric sodium atoms with two photons, using two lasers operating at 589nm and 569nm (case 2). We present a new method which consists in exciting the level 4P$_{3/2}$ with a single photon, using a laser operating at 330nm (case 1). Thanks to a modeless laser we show that 1W in case 1 produces the same flux as 30W in case 2. Moreover, to reach necessary flux at 330nm one needs 10W in case 1 whereas one would need more than

400W in case 2. This new method is very promising in terms of flux but also in terms of simplicity.

1. Introduction

Near-diffraction-limited imagery on very large telescopes has become a major tool in astrophysics. Adaptive optics (AO) allows these observations if a source, within the isoplanetism domain of the observed object is bright enough, to be able to analyze the incident wave surface. The probability to find such bright sources is the main limitation of AO, especially in visible range. To increase the sky coverage, large astronomical facilities use or will implement a monochromatic laser guide star (LGS)[1,2,3,4,5]. An important progress was achieved in 2004 on a 10 meters family telescope at Keck Observatory. This result showed[6] that AO works very well thanks to a 14th magnitude ($\sim 2 \times 10^4$ photons/s/m^2) natural guide star (that we call, in this paper, TTNGS from « tip-tilt natural guide star ») for tip-tilt correction and a 9.5[th] magnitude ($\sim 1.7.10^6$ photons/s/m^2) LGS for higher order corrections. This important result has become a reference. The corresponding experimental data will be used often in this paper. At Keck[7] Observatory, a 50cm diameter projector focuses in the mesosphere a 17W laser (on top of the telescope) at 589nm. LGS star provides the phase reference except for the slope θ, its position being indeterminate[8]. The natural TTNGS star is used to measure θ, and, as a result, another limitation appears: the probability to find a natural star bright enough is in the best case $\sim 10^{-7}$ in visible at the galactic poles[9]. The polychromatic laser guide star

(PLGS) resolves this major difficulty, by creating a multiple wavelengths radiating source which consist of the D_2 component corresponding to the LGS star and other UV-VIS-IR components that we call in this paper TTLGS from "tip-tilt laser guide star". The tip-tilt θ is measured via the differential tip-tilt $\Delta\theta$ between chromatic components. θ is proportional[10] to its derivative $\Delta\theta$ as a function of λ. The R&D ELP-OA program is probably the only one in the world to ensure 100% sky coverage. This is necessary for very faint astrophysic objects, the priority of 10 meters optical telescopes (DOT). The initial proposal to produce a PLGS consists in exciting the mesospheric sodium atom $4D_{5/2}$ level via the intermediate level $3P_{3/2}$, with two dependents lasers at 589nm and 569nm. This excitation with classical lasers raised the first problem of intrinsic atomic saturation of $3S_{1/2} \rightarrow 3P_{3/2}$ and $3P_{3/2} \rightarrow 4D_{5/2}$ sodium transitions. We overcome this first limitation by developing a modeless laser[11] that spread out the peak power over all velocity classes of the sodium atom vapour. Therefore we hope to gain at least a factor 10 on the returned flux. In spite of this gain, there is a risk that the returned flux is not sufficient for ELP-OA program. Indeed, the second limitation comes from the fact that the measurement of $\Delta\theta$, via the TTLGS chromatic components, has to be more precise than the direct measurement of θ, via the TTNGS natural star, that is essential in the case of a monochromatic laser guide star LGS. The proportionality factor[12] that links θ to $\Delta\theta$ is about 18. The TTNGS and TTLGS stars are measured in the full-field of view of telescope, thus the respective performances can be compared. As a result, photons flux of the TTLGS chromatic components should be 18×18 times more intense (ie of about 6 times fainter magnitude) than the TTNGS star photons flux. Keck's and Gemini's engineers[1,13] estimate that the magnitude m_v of natural star TTNGS cannot exceed 18th

magnitude ($\sim 7 \times 10^2$ photons/s/m^2) and that the magnitude allowing an acceptable AO operation is about 16 ($\sim 4 \times 10^3$ photons/s/m^2). In paper 7, authors achieved a Strehl ratio of 36% in K′ band using a 14th (2.6×10^4 photons/s/m^2) magnitude TTNGS. Recent[14] progress has shown that it is possible to achieve the same performance using a 16th magnitude. Thus we can see that the ELP-OA's TTLGS chromatic components magnitude has to be under 12 ($\sim 2 \times 10^5$ photons/s/m^2) and equal to 10 ($\sim 1.3 \times 10^6$ photons/s/m^2) for a good correction. Thus the TTLGS chromatic components have to be almost as intense as the LGS star, measured at Keck Observatory. This is a challenge that requires a precise study of the laser-sodium interaction. The initial proposition to produce a PLGS[10] star with two laser excitation at 589nm and 569nm does not allow this equalization. We demonstrate that the corresponding TTLGS chromatic components are 100 times fainter than the LGS D$_2$ component. Roughly, if the LGS star has a returned flux of about 10^6 photons/s/m^2 then, the TTLGS star components flux will be around 10^4 photons/s/m^2, that is extremely insufficient. If electronics and algorithms are still able to gain in sensitivity (a factor of 10 seems to be possible[15]), it remains to find a method to increase at least one order of magnitude TTLGS star flux.

Thanks to the remarkable properties of the modeless laser that we developed for ELP-OA, we report on, in this paper a solution that allows gaining a theoretical factor of 10. It consist in producing independent TTLGS and LGS, via a one photon direct excitation of $3S_{1/2} \rightarrow 4P_{3/2}$ Na transition at 330nm with a modeless laser. Only a modeless laser allows considering this possibility. From an instrumental point of view, this solution has an important advantage because it preserves the current LGS facilities, without any modification. Taking into account atmosphere transmission at 330 nm on the Keck's site

in Hawaii, we show that a 1W modeless laser at 330nm at the mesosphere (~2-3W at the ground) produces a TTLGS components returned flux identical with the one obtained by an excitation using two lasers of 2×15W (at the mesosphere) at 589nm + 569nm. A 10 times higher flux can be obtained with an about 10W modeless laser at 330 nm. More than 400W at 589nm +569 nm would be necessary to get this gain. Such high power is problematic on astronomical facilities. The new solution that we propose is simpler and cheaper. It allows spatially, temporally and spectrally uncoupling for both TTLGS and LGS stars and corresponding lasers. This simplification brings the whole laser guide star system more robust and reliable.

In this paper we compare, from the theoretical point of view, the photons flux of the radiative cascade generated by one photon excitation of $4P_{3/2}$ level at 330 nm of Na atom, with the one generated by two photons excitation of $4D_{5/2}$ level at 589 nm and 569 nm for different types of lasers.

2. The model

The model that we have used is similar to the one described in paper 11 for the $3S_{1/2}$ → $3P_{3/2}$ D_2 transition. We consider the two cases quoted above.

2.1 Case 1: $4P_{3/2}$ level one photon direct excitation at 330nm.

$4P_{3/2}$ level can be directly excited, from the ground state $3S_{1/2}$, with a laser centred at 30272.51cm^{-1} (~330nm). Figure 1 presents the energy levels involved in the radiative cascade of the process. The system of the rate equations that describes the atomic system is:

$$\frac{\partial N_1(t,\mathbf{r},v)}{dt} = -N_1(t,\mathbf{r},v)\frac{g_1}{g_5}\int_{-\infty}^{+\infty}\sigma(v'-v)\Phi(t,\mathbf{r},v')dv'$$

$$+\left(\frac{N_5(t,r,v)}{\tau_{51}}+\frac{N_2(t,r,v)}{\tau_{21}}+\frac{N_3(t,r,v)}{\tau_{31}}\right) \qquad (1)$$

$$+N_5(t,r,v)\int_{-\infty}^{+\infty}\sigma(v'-v)\Phi(t,r,v')dv'$$

$$\frac{\partial N_2(t,r,v)}{dt}=\frac{N_4(t,r,v)}{\tau_{42}}-\frac{N_2(t,r,v)}{\tau_{21}} \qquad (2)$$

$$\frac{\partial N_3(t,r,v)}{dt}=\frac{N_4(r,t,v)}{\tau_{43}}-\frac{N_3(t,r,v)}{\tau_{31}} \qquad (3)$$

$$\frac{\partial N_4(t,r,v)}{dt}=-\frac{N_4(t,r,v)}{\tau_{43}}-\frac{N_4(t,r,v)}{\tau_{42}}-\frac{N_5(t,r,v)}{\tau_{54}} \qquad (4)$$

$$\frac{\partial N_5(t,r,v)}{dt}=N_1(t,r,v)\int_{-\infty}^{+\infty}\sigma(v'-v)\Phi(t,r,v')dv'$$

$$-\frac{N_5(t,r,v)}{\tau_{54}}-\frac{N_5(t,r,v)}{\tau_{51}} \qquad (5)$$

$$-N_5(t,r,v)\frac{g_1}{g_5}\int_{-\infty}^{+\infty}\sigma(v'-v)\Phi(t,r,v')dv'$$

$$\sum_{i=1}^{5}N_i(t,r,v)=N_D(v)=N_1(t=0,r,v) \qquad (6)$$

where

$t = time\ (s)$

$r = vector\ of\ the\ radial\ position\ in\ the\ laser\ beam\ (m)$

$v = frequency\ Doppler\ shift\ (Hz)$

$g_1,\ g_5 = degeneracy\ of\ the\ 3S_{1/2}\ and\ 4P_{3/2}\ states\ respectively$

$1/\tau_{ij}$ = probability of the transition $i \rightarrow j$ (s^{-1})

Φ = laser photon flux density per unit area, unit time and unit frequency ($m^{-2}s^{-1}Hz^{-1}$)

σ = homogeneous absorption cross section (m^2)

N_i = population of the level i

N_D = Doppler distribution population assuming a uniform temperature at the mesosphere across the laser beam

The three terms of equation 1 correspond to absorption, spontaneous emission and stimulated emission. Using the same hypotheses as in paper 11, we define the spatial temporal saturation parameter as:

$$S(t,r,v) = \tau_{51} \int_{-\infty}^{+\infty} \sigma(v'-v)\Phi(t,r,v')dv' = \tau_{51}\varphi(t)D(r)\sigma_{eff}(v) \qquad (7)$$

The effective cross-section $\sigma_{eff}(v)$ is the convolution product of the homogenous absorption cross-section $\sigma(v)$ of sodium atom and the normalize laser line shape $g(v)$. The homogenous absorption has a Lorentzian profile:

$$\sigma(v) = \frac{\sigma_0(\Delta v/2)^2}{(v_0-v)^2+(\Delta v/2)^2} \qquad (8)$$

where σ_0 is the homogenous cross section centred at v_0, and v_0 is the frequency line center . Δv is the homogenous linewidth of the transition.

$D(r)$ is the laser photons flux distribution per unit of area. In order to reduce the calculation time, a commonly used approximation consists in taking $D(r)$ constant over the diameter $2w$ of the laser beam. In practice phase mirrors allow this spatial laser beam profile. We approximate the temporal laser linewidth $\varphi(t)$ as a rectangle function of linewidth τ_L. Consequently:

$$S(t,v) = N_L \frac{\tau_{51}}{\tau_L} \frac{\sigma_{eff}(v)}{\pi w^2} \qquad 0 < t < \tau_L$$

$$S(t,v) = 0 \qquad t < 0 \ et \ t > \tau_L \tag{9}$$

where $N_L = \dfrac{E}{h\nu}$ is the photons number in a laser pulse and $E = P_\lambda / f_L$ the pulse energy

(where P_λ is the mean laser power value at wavelength λ).

The Doppler distribution can be written as:

$$N_D(v) = N_D^0 \frac{2\sqrt{\ln(2)/\pi}}{\Delta v_D} e^{-(\frac{2\sqrt{\ln(2)}}{\Delta v}v)^2} \tag{10}$$

where $N_D^0 = \rho \Delta z^{-1}$ is the atomic density by unit of volume , ρ is the column density et Δz

is the column height.

2.2 Case 2: 4D$_{5/2}$ two photons excitation at 589nm and 569nm via 3P$_{3/2}$ level.

Figure 2 shows the system of excitation and the radiative cascade induced by two lasers

at 589nm and 569nm locked on the transitions 3S$_{1/2}$ → 3P$_{3/2}$ and 3P$_{3/2}$ → 4D$_{5/2}$. The

formalism used is the same as the one described above. Two effective cross sections are

involved σ_{01} and σ_{02} corresponding to *3S$_{1/2}$→3P$_{3/2}$* and *3P$_{3/2}$→4D$_{5/}$* transitions. We will

not describe here the rate equations system that is obvious.

3. Returned fluorescence photons flux

3.1 Calculation of returned flux

Neglecting non radiative processes, the fluorescence flux of the TTLGS chromatic

component corresponding to *i* towards *j* level transition is :

$$\Phi_{ij} = Tf_L \frac{A\Delta z}{4\pi z^2} \frac{1}{\tau_{ij}} \int_{-\infty}^{+\infty} dv \int_{-\infty}^{+\infty} d^2r \int_{pulse} N_i(r,t,v)dt = Tf_L \frac{A\Delta z}{4\pi z^2} \frac{1}{\tau_{ij}} \pi w^2 \int_{-\infty}^{+\infty} dv \int_{pulse} N_i(t,v)dt \tag{12}$$

Δz is the thickness and z is the height of the sodium layer, A is the receiver area at the ground (fixed to $1m^2$ in the following), T is the atmospheric transmission at the wavelength corresponding to the transition i→j and f_L is the lasers repetition rate.

The simulation was carried out for three types of laser lines $g(v)$:

1) **laser of type I** : a Gaussian inhomogeneous line shape of width $\Delta v_L=1MHz$ simulating longitudinal single-mode laser;

2) **laser of type II** : the same line as the previous one , followed by a double phase modulation at 180MHz and 325MHz in order to generate sidemodes;

3) **laser of type III** : a Gaussian inhomogeneous line shape of width $\Delta v_L=$ 2.8GHz (at $1/e^2$) for $3S_{1/2}$→$3P_{3/2}$ and $3S_{1/2}$→$4P_{3/2}$ transitions and $\Delta v_L=$ 1GHz for transition $3P_{3/2}$→$4D_{5/2}$; this spectral line shape simulates a modeless laser that excites all velocity classes of the sodium Doppler/Hyperfine profile[11]. It is well known that the hyperfine structure of $3S_{1/2}$ level is 1.77GHz.

The different atomic parameters used in this paper are summed up in table 1. In spite of few divergences found in the literature, the transitions probabilities $1/\tau_{ij}$ and homogenous absorption cross-section σ_0 and σ_{0i} have been taken equal to the one of reference 10.

Sodium density N_D^0 is the most important source of dispersion of experimental results. Indeed, Megie et al. showed[16] that seasonal variations of the sodium column density $\rho = \Delta z N_D^0$ is maximum in November-December, about $8x10^9$atoms/cm^2, and minimum in May-June, about 2×10^9atoms/cm^2, that is to say, a seasonal variation factor of 4. Sodium concentration can also depend on the site. Moreover, Kwon and al.[17] observed during the winter of 1987 at Mauna Kea Observatory (Hawaii), sodium sporadic of about 40min duration that produced sharp sodium abundance peaks of around

9

6.7×10^9 atoms/cm^2, whereas the mean value was around 3.5×10^9 atoms/cm^2. A detailed study was carried out by Michaille et al.[18] at La Palma from September 1999 to August 2000 and showed that the sporadic probability events is about 1 per night, on a time scale going from a few seconds to a few hours. The authors concluded that the origin of the sporadic is still uncertain and that adaptive optics operation will not be affected, in terms of defocusing. The mean value of sodium column density measured by the authors at La Palma is about 4×10^9 atoms/cm^2. Gardner et al[19] also showed that tropospheric gravity waves propagate in the mesosphere creating spatial modulation full the sodium column density able to modify the local value by 100% in a few hours. In conclusion, all the results found in the literature, show that the mean value of the sodium column density is

$\rho \approx 4 \times 10^9 \, atomes / cm^2$ ($N_D^0 = 4 \times 10^9 \, atomes / m^3$ for a column height of $\Delta z = 10 km$).

As Φ_{ij} is proportional to the column density $\rho = \Delta z N_D^0$, the value of Δz does not have any effect in the calculation that we present in this paper.

We wrote a numerical program using MATLAB. Neglecting the coherence effects, the following calculations are taking into account each frequencies ν with a step of $\Delta\nu =$ 1MHz. The convergence process has been approached very carefully. The numerical calculation of population state has been carried out with an adaptive step integrator. The initial population condition has been given for each frequencies ν, by the distribution $N_D(\nu)$.

3.2 Required flux

To estimate the required flux, we have used the results concerning LGS star and TTNGS star magnitude published by Keck[6,7]. Until now, this is the only full experimental set-up

that is working on a 10m telescope facility. A LGS star of magnitude $m_V^{LGS} = 9.5$ has been obtained with 10 to 20W laser power (typically 17W) on top of the telescope. Taking into account atmospheric losses we estimate that 15W is projected in the mesosphere. As we said above good tip-tilt correction is ensured by a natural TTNGS star of magnitude $m_V^{TTNGS} \approx 16$. It is more convenient to work in terms of number of photons per second and unit area. Consequently, the following conversion[20] is used:

$$m_V = -2.5 \log_{10} \frac{\Phi}{\Phi_0} \tag{11}$$

With Vega as reference star, $\Phi_0 = 2.54 \times 10^{-10} \; lumens.cm^{-2}$, i.e. in band V centred at 555nm $\Phi_0 = 1.043 \times 10^{10} \; photons/s/m^2$.

Thus we calculate for the LGS and TTNGS stars:

$$m_V^{LGS} = 9.5 \Rightarrow \Phi_{LGS} = 1.7 \times 10^6 \; photons/s/m^2$$
$$m_V^{TTNGS} = 16 \Rightarrow \Phi_{TTNGS} = 4.2 \times 10^3 \; photons/s/m^2 \tag{12}$$

The tip-tilt correction requires a natural guide star TTNGS of a relatively weak intensity. But, the UV-VIS-IR chromatic components of TTLGS star needs much larger intensity. Indeed, the relation between the tip-tilt θ and the differential tip-tilt $\Delta\theta$ is:

$$\theta = \frac{n_3 - 1}{n_2 - n_1} \Delta\theta \approx 18 \times \Delta\theta \tag{13}$$

where n_3 is the average value of the air refraction index at the observation wavelength and n_2 and n_1 are the indexes of the TTLGS chromatic components. The measurement of $\Delta\theta$ has to be 18 times more precise than the measurement θ. Assuming photons noise limitation, the intensity of the TTLGS chromatic components has to be $18^2 = 324$ times more intense than the intensity of the TTNGS star. The required photon flux is therefore:

$$\Phi_{TTLGS} = 324 \times \Phi_{TTNGS} \approx 1.4 \times 10^6 \ photons / s / m^2 \approx \Phi_{LGS}$$

I.e. the intensity of the UV-VIS-IR chromatic components of the TTLGS must be the same order of magnitude as the LGS star intensity (D_2 component). We show below that this is impossible using case 2 (two photons excitation at 589nm + 569nm).

We conclude that a TTLGS chromatic component flux of about 10^6 photons/s/m^2 at 330nm is necessary for the ELP-OA project.

3.3 Validation of the model based on Keck, PASS-2 and PASS-1 experimental results

To reproduce the photons flux of the LGS star obtained at Keck, we have run our simulation program for case 2, considering the power of the second laser $P_{569}=0$, $f_L=11kHz$ and $\tau_L=100ns$. The mean sodium column density has been taken equal to the one measured at Mauna Kea Observatory ($\rho = 4 \times 10^9 \ atomes / cm^2$). Taking into account the atmospheric transmission in Hawaii, the laser power P_{589} at the mesosphere at 589 nm was equal to about 15W. The waist value $w= 0.4m$ (see below) has been taken in order to be compatible with the measurements of Keck's LGS star shape[Erreur ! Signet non défini.].

Figure 3 displays the result for the three types of lasers presented above. We notice the favourable evolution of the intensity of the LGS star when using from a single mode laser to a modeless laser, via a phase modulated laser. This behaviour was already experimentally measured and theoretically calculated. Our calculation gives a LGS flux of 1.6×10^6 photons/s/m^2 for the experimental conditions of Keck Observatory. This value has an excellent agreement with the measurement of Keck $m_V\sim9.5$ (1.7×10^6 photons/s/m^2).

In the ELPOA project, the sky photometry experiment of PASS-2 Pierrelatte/France[21,22,23] provided a photon flux at 330nm versus the laser power at 589nm and 569nm, for types I and II lasers. Table 2 and figures 4 and 5 compare the experimental results of PASS-2 with our theoretical calculation of case 2, with P589=P_{569}. The sodium column density during PASS-2 experiment was not measured. Then, the calculation of the Φ_{51} flux at 330nm was carried out for a mean sodium column density of $\rho = 4 \times 10^9 \ atomes / cm^2$. Lasers power for PASS-2 experiment is taken at the ground. Thus for lasers beams attenuation, the atmospheric transmission equal to *T=0.8* has been used. The experimental values considered are average values of the published results, corresponding to a total laser power at the ground *P=P_{589}+P_{569}* of about 20W and 100W for type II laser and 14W for type I laser. At the ground, the near-diffraction lasers beams area is a rectangle of 28×35mm^2. To keep the same near diffraction area at the mesosphere and using the laser shape definition of our calculation, we have considered a waist *w* of 1m. A factor better than 2 is obtained for PASS-2 experiment, between the experiment and our calculation (see table 2 and figures 4 and 5), that is a very good agreement, according to the hypothesis and experimental conditions.

The photometry experiment of PASS-1[24] has been achieved with LLNL lasers (ALVIS project), in case 2. The laser experimental set-up is described in paper **Erreur ! Signet non défini.**. Table 3 summaries the well-known experimental parameters. Taking into account the atmospheric transmission at LLNL, the laser average power at the mesosphere *P=P_{589}+P_{569},* is estimated equal to 280W during the experiment. The variables parameters have been: the repetition rate (4.3-12.9 kHz), the laser power ratio $P_{569} /(P_{589} + P_{569})$ (30%, 50% and 70%), and the laser linewidth at 589nm (1-3GHz).

The set of results has shown a Φ_{51} returned flux at 330nm that presents little variations between 2.1×10^5 photons/s/m^2 and 5.1×10^5 photons/s/m^2 (figure 4 of paper 24). We lead our calculations for lasers type II and III, a sodium column density $\rho = 4.1 \times 10^9\ atomes/cm^2$ and the laser power ratio 30%, 50% and 70%. In PASS-1 experiment the laser beam area at the mesosphere is supposed to be of about 1m^2 with a Fried parameter r_0 of 6cm; this corresponds for our model to a beam waist w of 0.56m. But in paper 25, the measured area beam of the same experimental set-up was 3.14m^2 which gives a waist w of 1m. The knowledge of the beam area is critical because with 280W of laser power the saturation of the sodium transitions involved is strong, even with modeless lasers. Table 3 shows the calculation with w=0.56m for type II and III laser and with w=1m for type III. This result displays clearly that the laser used at LLNL was equivalent to a type III laser, i.e. that the laser linewidth covered continuously the sodium Doppler/Hyperfine profile. The ALVIS lasers remained confidential, we do not know what kind of « modulator » and applied voltage was used, but we believe that the LLNL lasers, had the same efficiency as our modeless laser, i.e. all sodium velocities classes in the mesosphere were excited as it supposed in paper 24. The last column of table 3 shows a very good agreement between the experimental results and our theoretical approach. For waist w=1m and type III lasers of 280W total mean power the returned flux is about 3×10^5 photons/s/m^2.

As a result, we can already conclude on two points: i) the experimental LGS and PLGS flux measured at Keck, PASS-1 and PASS-2 validates our model; ii) two 589nm and 569nm modeless lasers (type III) of total power *P=280W* (at the mesosphere) will produce a returned flux at 330nm between 2×10^5 photons/s/m^2 and 5×10^5 photons/s/m^2.

This flux is close to the one required (see section 3.2) but, with laser powers which can hardly be installed at an astronomical telescope.

3.4 Returned flux comparison between case 1 and 2.

In the following, the repetition rate and the laser pulse width were fixed at the current nominal values of ELP-OA project: f_L= 17kHz and τ_L= 50ns. Like we said before, the laser beam spatial shape $D(r)$ is approximated as a rectangular function, with the circular waist w. The different international LGS and PLGS projects recommended a 50cm diameter projector for a good astronomical site (r_0~10cm at 500nm). Therefore, in this paper the waist value w has been chosen in order to be compatible with Keck measurement of the full width half maximum LGS angular diameter α=1.4 arcsec obtained with a 50cm diameter projector and a near-diffraction laser beam. According to the spatial shape definition considered in our calculation, the waist is:

$$w = \frac{tg(\alpha).z}{2\sqrt{\ln(2)}} \approx 0.4m \ .$$

Figure 6 displays the photon flux Φ_{51} at 330 nm in case 1 (curves 4, 5, 6) and 2 (curves 1, 2, 3). The flux for the other TTLGS wavelengths can be deduced as follows:

$$\Phi_{51} = \frac{1}{2}\Phi_{54} = \Phi_{43} = \Phi_{42} = \Phi_{21} \text{ in case 1 and 2, and} \Phi_{51} = \Phi_{31} \text{ in case 1. In case 2, D}_2$$

transition flux Φ_{31} is essentially due to the one photon excitation-relaxation process at 589nm (LGS). In figure 6, P corresponds to the total laser power on top of the telescope $P_{589}+P_{569}$ with $P_{589}=P_{569}$ in case 2, or to the UV laser power P_{330} in case 1. Considering that the atmospheric transmission is strongly dependent on the astronomical site, the lasers powers used in section are the one at the mesosphere. The power 30W-VIS

corresponds to current ELP-OA project; i.e. two 20W lasers of type III at 589nm and 569nm at the ground. Table 4 summaries the different possibilities. In both cases 1 and 2, the modeless laser (type III) gives the best results, because the laser transitions considered are strongly saturable. The saturation intensities involved are:

$$3S_{1/2} \rightarrow 3P_{3/2} : I_{13}^{Sat} = \frac{h\nu_{589}}{\sigma_{01}\tau_{31}} \approx 185W/m^2$$

$$3P_{3/2} \rightarrow 4D_{5/2} : I_{36}^{Sat} = \frac{h\nu_{569}}{\sigma_{02}\tau_{63}} \approx 450W/m^2$$

$$3S_{1/2} \rightarrow 3P_{3/2} : I_{15}^{Sat} = \frac{h\nu_{330}}{\sigma_{0}\tau_{51}} \approx 45W/m^2$$

For these three transitions, if the whole laser power of respectively 15W, 15W and 1W excites only one velocity class, a saturation parameter of respectively: 190, 78 and 52 is obtained.

Table 4 shows the flux gain γ for different situations versus the normalised situation C_1 (case 2, two single-mode type I lasers of 2×15W). A gain γ of 11 is obtained in case 2 with two modeless lasers of 2×15W (see C_3 of table 4). It is a significant result. But remarkable result is that the same gain γ is obtained with only 1W at 330 nm of a modeless laser in case 1 (see C_6). Figure 7 emphasizes this important result versus laser power. Consequently, the modeless laser allows considering with great interest the 330nm sodium excitation which was rejected in paper 10 probably because of the strong saturation induces with a single-mode excitation (see C_4 of table 4). Figure 6 displays the evolution of the photon flux at 330nm Φ_{51}. A flux Φ_{51} of 4.2×10^4 photons/s/m^2 can be obtained in case 2 with two type III lasers of 2×15W at 589nm and 569nm, and in case 1 with one type III laser of only 1W at 330nm (see C_3 and C_6 of table 4). This flux is insufficient. But, we can see on figure 6 that, in case 1, the average slope is $\eta_1=3\times10^4$

photons/s/m^2/W whereas, in case 2, it is $\eta_2=1.3\times10^3$ photons/s/m^2/W, i.e. 20 times larger. This very encouraging result shows that 10W at 330nm (case 1) is enough to produce a flux of 3×10^5photons/s/m^2 whereas 400W at 589nm and 569nm (case 2) produces only 1.8×10^5photons/s/m^2 (see C$_7$ and C$_8$ of table 4). This last power cannot be implemented on an astronomical site, whereas 10W at 330nm is much easier. The UV star being absolutely necessary for PLGS, because is situated in a strong atmospheric dispersion wavelength region, case 2, initially considered, would need a large effort in order to reach the required specifications of section 3.2. Fundamentally, the reason comes from the fact that, in case 2, the flux Φ_{51} at 330nm is at least two orders of magnitude smaller than the flux Φ_{31} at 589nm (D$_2$). Figure 8 displays the ratio evolution Φ_{31}/Φ_{51} ($=\Phi_{D2}/\Phi_{330}$) versus P, in case 2 and for three lasers types' I-II-III. For the value 30-VIS in figure 6, that corresponds to the current ELP-OA program, using two modeless lasers of 2x20W (2x15W in the mesosphere), the theoretical flux Φ_{51} at 330nm and Φ_{31} at 589nm are respectively 4.2×10^4 photons/s/m^2 and 4.4×10^6 photons/s/m^2. The flux ratio Φ_{D_2}/Φ_{330} of ~105 is an intrinsic property of sodium atom.

4. Discussion

In the following, we consider the most favourable situation, corresponding to type III laser with ELP-OA characteristics.

4.1 Case 2: two photons excitation

The pulsed delay and the power balance between the two lasers can be optimized. Figure 9 shows an optimum delay of 3.7ns. A 10% gain is expected, but lasers temporal jitter of a few ns implies gain losses of same order of magnitude. Likewise, figure 10 shows an

17

optimum gain of 10%, when the power is distributed as a ratio of 35% on 589nm laser and 65% on 569nm laser (case P=30W). These gains are not sufficient to justify an extra cost of development.

It was shown during PASS-2 experiment that the radial superposition of the two lasers beams was not better than 10 %. This implies a flux decrease of 20%. Moreover, this superposition will be difficult to realise, when the two lasers will have to follow the observation star. Indeed, we will have to consider the prism effect of the atmosphere that must be compensated in real time when the laser beam is launch out of zenith. This is a major complication.

Without AO on laser emission the two lasers spots at the mesosphere have a speckle structure when the beam size in the low atmosphere is larger than r_0. The speckle structure that is a function of wavelength is different for each wavelength. As a result, the efficiency of the two photons excitation could decreases dramatically.

As seen before, case 2 would need lasers powers of hundreds of watts. Although the wavelength at 589nm can be produced using solid state lasers (frequency addition of two YAG[26] lasers or two fibre[27] lasers, Raman[28] laser…), no solid state lasers can generate 569nm. For the moment only dye lasers allow these wavelengths with high powers and high efficiency. The isotopic separation programs have demonstrated that is possible to obtain 1000W around 589nm and 569nm[29]. Moreover, around 100W, the modeless laser starts again to raise the problem of the saturation of sodium atom transitions.

Therefore, we see that in case 2, they are several difficult technical limitations and there are little possibilities to increase significantly the flux of the chromatic components of the TTLGS star. An incoherent excitation in case 2, with type III lasers allows a maximum

population transfer of 7% for 2×15W and 17% for 2×200W in $4D_{5/2}$ state. Only a coherent excitation, with a theoretical transfer of population of 100% in $4D_{5/2}$ state could allow a significant gain[30]. This solution is definitely very difficult to implement on the sky and on an astronomical site, because it requires ultra-fast lasers, with energies per pulse of about few $\mu J/cm^2$ that imply, at the mesosphere, mean power approaching 100W with required spot size and lasers repetition rate. Many technical problems will probably imply a transfer significantly weaker than 100%.

4.2 Case 1: one photon excitation

The direct excitation of $4P_{3/2}$ at 330nm (case 1) is more promising for several reasons. First, this solution is fundamentally more efficient, because only one laser of type III of 1W allows a transfer of 3% in the sodium state $4P_{3/2}$ and 20% for 10W. It is well known, that assuming a two levels absorption transition, the maximum population transfer can be 50% in the case of an incoherent excitation. Let us recall that a flux Φ_{51} of 3×10^5 photons/s/m^2 is achieved in the conditions defined in section 3.2: laser of type III of 10W (in the mesosphere), f_L=17kHz, Δt=50ns, w=0.4m, ρ=4×10^9atoms/cm^2. Many parameters can allow the optimization of the returned flux. For example, a cw laser of 10W at 330nm would give a photons flux Φ_{51} of 1.1×10^6 photons/s/m^2 (see C_9 of table 4). This value is much larger than the flux value Φ_{51} of 4.2×10^4 photons/s/m^2 obtained from two lasers of 2×15W (in the mesosphere) of type III for current ELP-OA project.

Despite the weaker atmospheric transmission at 330nm on a good astronomical site (40%-50% instead of 80%), a modeless laser 2-2.5 W (at the ground) is enough to equal the current solution considered for ELP-OA project, and a modeless laser of 20-25W for a flux 10 times more intense. Contrary to 589nm and 569 nm, for 330nm it exist efficient

19

solution of solid states lasers. Quasi-cw laser of 10W at 355 nm with $M^2 < 1.2$ is already in sale. There are solid state systems such as: Nd :YAG pumped by laser diodes and frequency tripling[31]. Nd doped YAG or YLF matrix has intense laser line at 1321nm. Nd :YLF has its maximum gain at 1321nm. Using frequency quadrupling we can obtain in the previous case the laser line at 330nm[32]. There are also high power optical fibers lasers at 1321nm [33]. We can also realise frequency addition of frequency doubling of a 532nm Nd :YAG with a 870nm Sa :Ti laser or a high power laser diodes. UV laser diode progress is promising. Laser diode working directly at 375 nm is in sale. Other solutions already exist. While waiting for this kind of solid sources development, we can easily use a frequency doubling high yield DCM dye laser at 660nm, to obtain power higher than 10 watts at 330 nm.

Another important advantage is the simplification on an astronomical site. The solution that we propose does not modify monochromatic laser guide star facility (LGS) that is working on very large telescopes. For tip-tilt correction it is sufficient to replace the TTNGS star by TTLGS star produced by an independent laser at 330nm. The TTLGS star can be positioned anywhere in the isoplanetism field. It is not necessary to extract the superimposed component D_2 and at least two UV-VIS-IR components of the PLGS star. This is a gain in simplicity and yield. For example, no grating is needed to extract the D_1 and the D_2 components, as in the case of PASS-1 and PASS-2. Furthermore in case 2, D_2 line has two components: one comes from the one photon excitation at 589nm (LGS) and the other one from the radiative cascade (TTLGS) (see figures 1 and 2). The last one would be useful to measure $\Delta\theta$. However they cannot be separated. Thus, to measure $\Delta\theta$

in case 1, D_2 component can be used together with D_1 component, that doubles the returned flux at 589 nm and eliminates the use of a grating.

The technical problems of spatial superposing and time synchronisation evoked above disappear because the two lasers that produce TTLGS and LGS are independent. This means a better reliability. An additional flexibility is the choice of lasers repetition rate. Indeed, the atmospheric coherence times of the wave front and of the tip-tilt are:

$$\tau_{0,wavefront} = r_0 / \Delta v \tag{14}$$

$$\tau_{0,tilt} = 12.33 \left(\frac{D}{r_0} \right)^{1/6} \left(\frac{r_0}{v} \right) \tag{15}$$

r_0 is the Fried parameter, D the telescope diameter and v the wind velocity. In visible range ($\sim$0.5µm) and for telescopes of 8-10m range, $\tau_{0,wavefront}$ and $\tau_{0,tilt}$ are about to 10 ms and 100ms. As a result, the laser at 330nm that produces TTLGS star can have a repetition rate of 10 times weaker than the one at 589 nm used for high orders correction. This possibility can be interesting. For example, in order to increase the returned flux, $4P_{3/2}$ direct excitation could also be produced by an ultra fast laser for 100% transfer of the ground state population to the excited state $4P_{3/2}$ using laser coherent transfer or chirped laser adiabatically transfer. The essential point for a 100% transfer is the required energy per pulse which must be of the order of few µJ/cm^2. At 17 kHz repetition rate this implies huge mean laser power (850W for a 1m^2 spot, 5µJ/cm^2 and repetition rate of 17 kHz). Then, we could think that the laser repetition rate can be decreased until it becomes inversely proportional to the time of coherence of the tip-tilt, in order to reach the required energy per laser pulse for the same average power. However, in terms of photon flux per second it is clear that to keep a 100% population in the excited state for each

laser pulse during time dt at 1kHz is equivalent to maintain a 10% population during time dt at 10kHz. The cost and technical difficulties determine the choice.

Another question is the angular extension of the laser beam versus wavelength. Atmospheric turbulence limits the beam propagation. The Fried parameter r_0 varies with wavelength: $r_0 \propto \lambda^{6/5}$. An average value of the Fried parameter r_0 at a good astronomical site is about 10cm at 589nm and 5cm at 330nm. If the laser beam size is close or larger then the angular spot size is limited by the seeing λ/r_0. The seeing varies slowly with λ as $\lambda^{-1/5}$. This means, that a spot size at the mesosphere needs a projector of approximately the same diameter at 589-569nm and 330nm.

If the noise in measuring $\Delta\theta$ was dominated by the Rayleigh residual scattering of atoms and molecules of the higher atmosphere observed in the telescope field of view, we could think that the solution presented in case 1 would be worse from this point of view. However, this is not the case. Indeed, the Rayleigh scattering increases like: $\eta_R = \dfrac{P_{330}}{P_{589}}\left(\dfrac{\lambda_{589}}{\lambda_{330}}\right)^4$. Case 1, involving less power laser, is in fact more convenient. For 1W at 330nm and 30W at 589nm+569nm η_R is 0.3 and for 10W at 330nm and 400W at 589nm+569nm η_R is 0.25. For an identical returned flux, the Rayleigh scattering is thus 3 or 4 times weaker in case 1. Moreover, we will demonstrate in a future paper that thanks to the modeless laser, the Rayleigh scattering can be eliminated.

Finally, one may expect that, on the new generation telescopes, the telescope vibration will be negligible and the optical axes will be stable. As a result the UV beam could be projected at the mesosphere by the telescope itself. Thus, the measurement of $\Delta\theta$ will not require the measurement of the gravity centre of the UV component of TTLGS because,

thanks to the light principle of reverse return light, the gravity centre of the UV component will not move. The measurement of only one VIS or IR chromatic component will thus be enough. This will represent a gain factor of 2 in the calculation time and an additional simplification in the optical system of observation.

5. Conclusion

The calculations using the model presented in this paper are in very good agreement with the experimental results on the sky of Keck, the LLNL and Pierrelatte. Our model clearly shows that the new solution suggested (case 1) which consists in exciting the sodium atom with one 330nm photon needs only 1W of a modeless laser to produce a returned flux of 4.2×10^4 photons/s/m^2 at 330nm. This flux is equivalent to that obtained by an excitation with two photons using two modeless lasers operating at 589nm and 569nm of 15W each (case 2). The flux which is required for the differential measurement of the tip-tilt θ is the main issue addressed in this paper. Taking the coherence time of the atmospheric tip-tilt into account, θ must be corrected at a frequency close to 100Hz. Under these conditions only a measurement of the centre of gravity of the chromatic components of TTLGS allows such a frequency. Preceding flux is then largely insufficient because one would have only a few hundreds of photons for the measurement of the centre of gravity which must be of an extreme precision. We showed that a returned flux at 330nm ranging between 2×10^5 photons/s/m^2 and 1.3×10^6 photons/s/m^2 is necessary. Our calculations clearly show that a modeless laser or quasi-continuous laser of 10W operating at 330nm makes it possible to fill the schedule of conditions whereas

one would need more than 2×200W at 589nm + 569nm. In order to validate this proposal, experiments in laboratory are in progress.

The solution suggested has also other advantages:

1. Two completely independent lasers at 330nm and 589nm leave a richer technological choice. All solid state lasers are then possible. One of the major disadvantages of case 2 is the wavelength at 569nm which does not have, to our knowledge, any solid state laser solution. It thus imposes dyes lasers for the two wavelengths because they must have rigorously identical characteristics.

2. The independence of LGS and TTLGS simplifies the system largely and allows an up-grade without deep modification of the existing LGS. The problems of tip-tilt and higher orders corrections can then be optimized more easily and separately. To obtain a sufficient intensity at 330nm, case 2 would require a power of more than 200W for the 589nm laser. But, such a power is useless for the production of LGS. 20W are enough.

3. The 330nm laser power to be implemented is relatively low and thus one can already consider very compact solid state systems which would be fixed directly on the telescope. It would not be then necessary to transport the beam any longer.

Table caption

Tab. 1.

Mesospheric sodium atoms parameters.

Tab. 2.

Parameters of the PASS-2 experiment and simulation. The lasers powers indicated for PASS-2 are ground powers. T is the atmospheric transmission at 589nm and 569nm which is supposed to be 0.8 at Pierrelatte.

Tab. 3.

Parameters of the PASS-1 experiment and simulation. See text.

Parameter	Case 1	Case 2	Unit
τ_{21}	32	32	ns
τ_{31}	16	16	ns
τ_{42}	40	40	ns
τ_{43}	40	40	ns
τ_{51}	320	320	ns
τ_{54}	160	160	ns
τ_{63}	-	75	ns
τ_{65}	-	150	ns
σ_0	4.10^{-14}	-	m^2
σ_{01}	-	$1.14.10^{-13}$	m^2
σ_{02}	-	$1.47.10^{-14}$	m^2
Δz	10^4	10^4	m
z	9.10^4	9.10^4	m

Table 1

	PASS-2			This work		
Laser type	II	II	I	II	II	I
f_L (kHz)	5					
τ_L (ns)	35					
w (m)	1					
$\rho\ (atoms/cm^2)$	NC			4×10^9		
$P=P_{589}+P_{569}$ (W)	~20	~100	~14	20×T	100×T	14×T
Φ_{330} (photons/s /m^2)	4800	26000	2400	8500	18300	2900

Table 2

	PASS-1	This work	This work	This work
Laser type	NC	II	III	III
f_L (kHz)	4.3-12.9	12.9		
τ_L (ns)	32			
$\Delta\nu_L$ (GHz) at 589nm	1-3	3		
$\Delta\nu_L$ (GHz) at 569nm	1	1		
$\rho\ (atoms/cm^2)$	4.1×10^9	4.1×10^9		
w (m)	0.56	0.56	0.56	1.0
$P=P_{589}+P_{569}$ (W)	290			
Φ_{330} (photons/s /m^2) $P_{569}/(P_{589}+P_{569})=30\%$	$2.1\text{-}4.2\times10^5$	2.5×10^4	1.2×10^5	2.5×10^5
50%	$2.0\text{-}5.1\times10^5$	3.1×10^4	1.3×10^5	3×10^5
70%	$2.8\text{-}4.0\times10^5$	3.6×10^4	1.4×10^5	3.2×10^5

Table 3

	C_1	C_2	C_3	C_4	C_5	C_6	C_7	C_8	C_9
Laser type	I	II	III	I	II	III	III	III	CW
f_L (kHz)	17								-
τ_L (ns)	50								-
$\rho\,(atoms/cm^2)$	4×10^9								
w (m)	0.4								
$P=P_{589}+P_{569}$(W)	30			-			400	-	-
$P=P_{330}$(W)	-			1			-	10	10
Φ_{330}(photons/s /m^2)	4×10^3	8×10^3	4.2×10^4	3.4×10^3	1.2×10^4	4.2×10^4	1.8×10^5	3×10^5	1.1×10^6
$\gamma\ (C_i/C_1)$	1	2	11	0.85	3	11	45	75	275

Table 4

Figure captions

Fig. 1.

Energy diagram and relaxation pathways of the one photon excitation of the $4P_{3/2}$ sodium

level at 330nm (case 1).

Fig. 2.

Energy diagram and relaxation pathways of the two photons excitation of the $4D_{5/2}$

sodium level at 589nm+569nm (case 2).

Fig. 3.

Returned fluorescence flux at 589nm (Φ_{31}, LGS) versus average laser power (at the

mesosphere) with Keck's laser characteristics for three types of lasers: i) 1 MHz single

longitudinal mode (dashed), ii) 1 MHz single longitudinal mode followed by a double

phase modulation at 180MHz and 325MHz (dashed point), iii) modeless (solid). The

arrow corresponds to the typical laser power and returned flux of Keck Observatory. This

calculation corresponds to case 2. It shows a gain of 6 between single mode and modeless

excitation.

Fig. 4.

Returned flux at 330nm of PASS-2 experiment at CEA Pierrelatte (see paper 23) versus

the peak power at 589nm ($=\dfrac{P_{589}}{f_L \tau_L}$) and total mean power ($P_{589}+P_{569}$). The dots

correspond to the experimental results using type II lasers and the solid curve

corresponds to the numerical simulation in case 2 with a column sodium density of

4×10^9atoms/cm^2.

Fig. 5.

Experimental and simulation of PASS-2 with type I lasers.

Fig. 6.

Return fluorescence flux at 330nm versus average laser power for the three types of lasers: a) 1 MHz single mode laser (curves 1 and 4), b) 1 MHz single mode laser followed by a double phase modulation at 180MHz and 325 MHz (curves 2 and 5) and c) modeless laser (curves 3 and 6). Solid curves correspond to the one photon excitation at 330nm (case 1) and dashed curves to the two photons excitation at 589nm + 569nm (case 2). The cross at 30W-VIS on the curve 3 corresponds to the ELP-OA project. The cross at 1W-UV on the curve 6 corresponds to the UV laser power at 330nm that equalize the flux of photons of the ELP-OA project. The cross at 10W-UV on the curve 6 corresponds to the flux that is closed to the required flux. 10W in case 1 gives 12 times more flux than 30W in case 2.

Fig. 7.

Ration between the returned flux at 330nm for a modeless laser excitation and for a single mode laser in the two cases as a function of laser power. Case 1: one photon excitation (solid curve). Case 2: two photons excitation (dashed curve).

Fig. 8.

Ratio evolution between the returned flux at 589nm and 330nm as a function of total laser power in case 2 and for the three types of lasers: i) type I - 1 MHz single mode laser (dashed), ii) type II - 1 MHz single mode laser followed by a double phase modulation at 180MHz and 325 MHz (dashed point) and iii) type III - modeless laser (solid). The cross
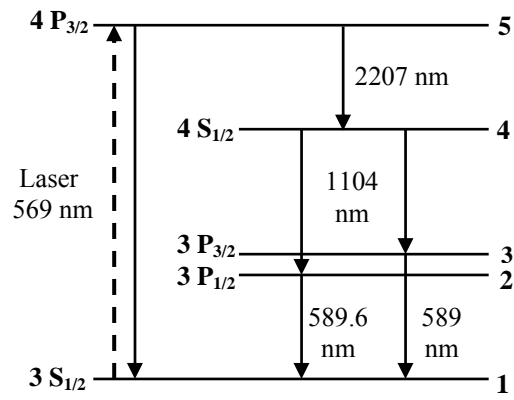
indicates that at 30W total laser power (ELPOA) the returned flux at 330nm is at least two orders of magnitude smaller than the one at 589nm.
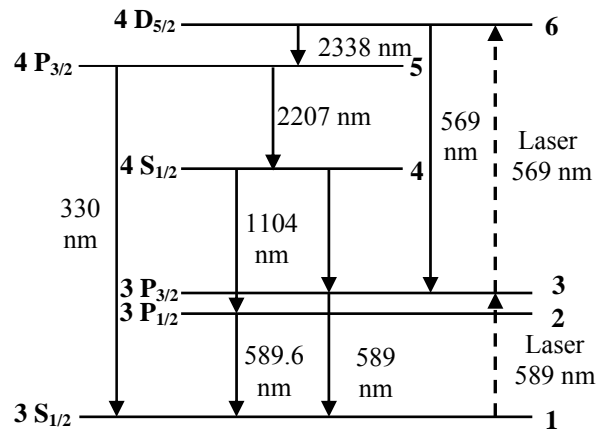
Fig. 9.

Returned flux at 330nm as a function of the delay between the 589nm and 569nm pulses in case 2. A gain of 10% is expected for a 3.7ns delay. Total lasers power is 30W.
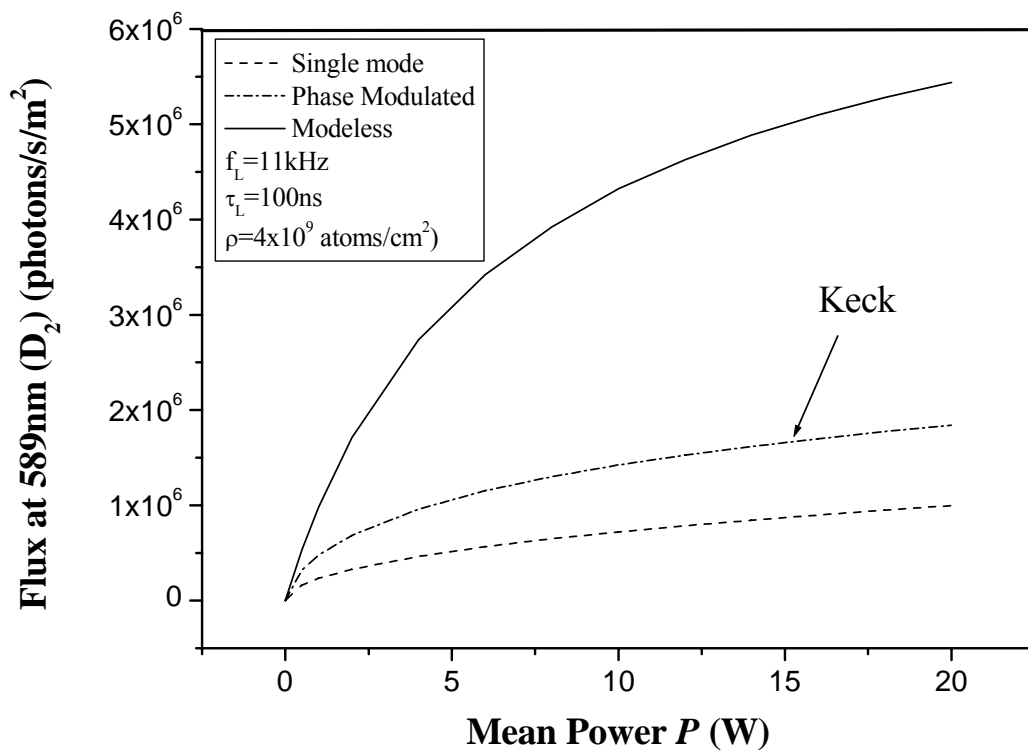
Fig. 10.

Returned flux at 330nm as a function of the ratio between 589nm laser power and total lasers power (589nm + 569nm) in case 2. A gain of 10% is achieved when the power is distributed as a ration of 35% at 589nm and 65% at 569nm. Total lasers power is 30W.
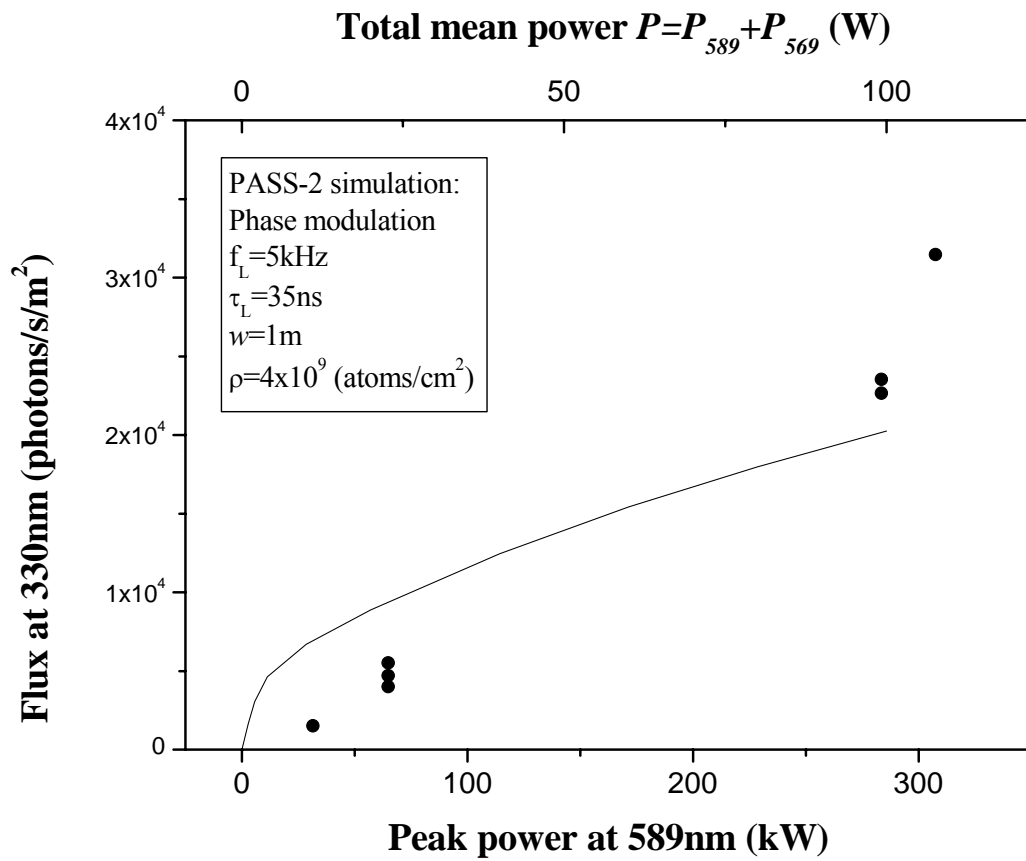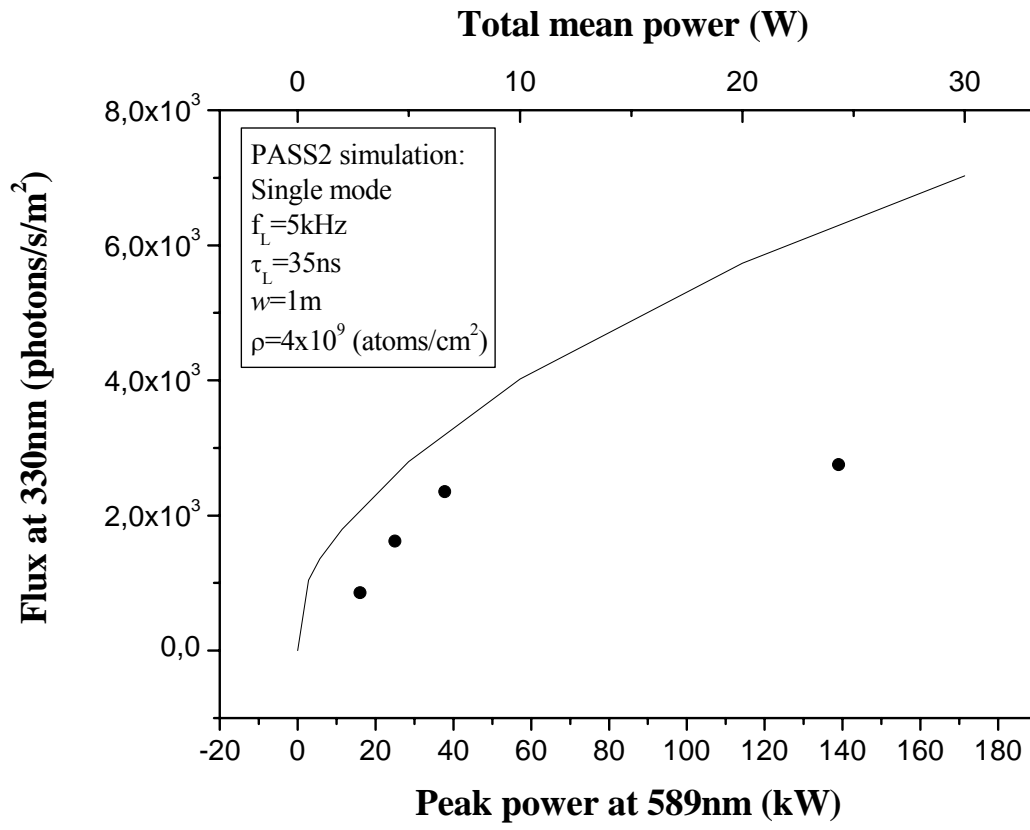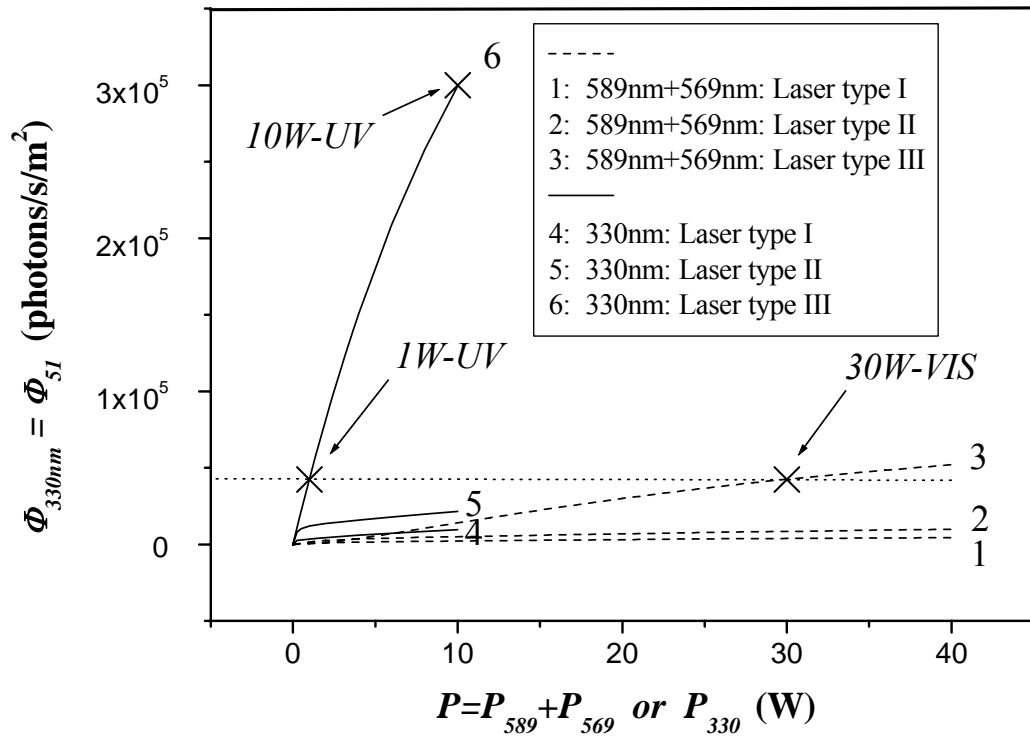
Figure 1

Figure 2

Figure 3

Total mean power $P=P_{589}+P_{569}$ **(W)**

Flux at 330nm (photons/s/m^2)

PASS-2 simulation:
Phase modulation
f_L=5kHz
τ_L=35ns
w=1m
ρ=4x10^9 (atoms/cm^2)

Peak power at 589nm (kW)

Figure 4

Total mean power (W)

Peak power at 589nm (kW)

PASS2 simulation:
Single mode
f_L=5kHz
τ_L=35ns
w=1m
ρ=4x10^9 (atoms/cm^2)
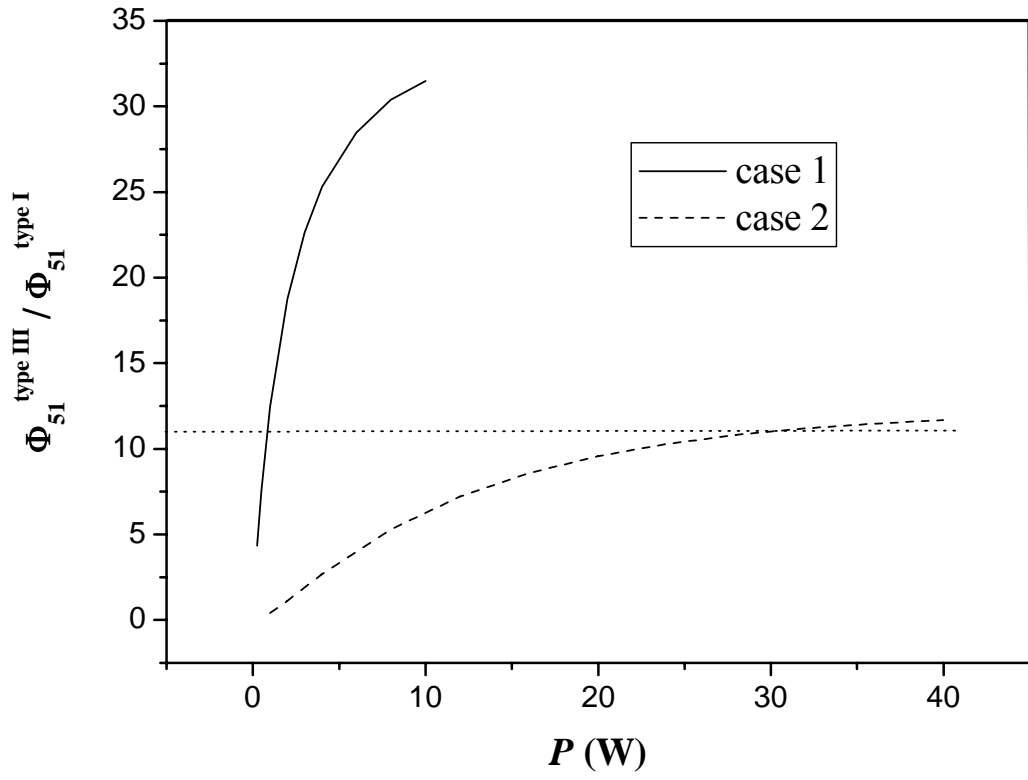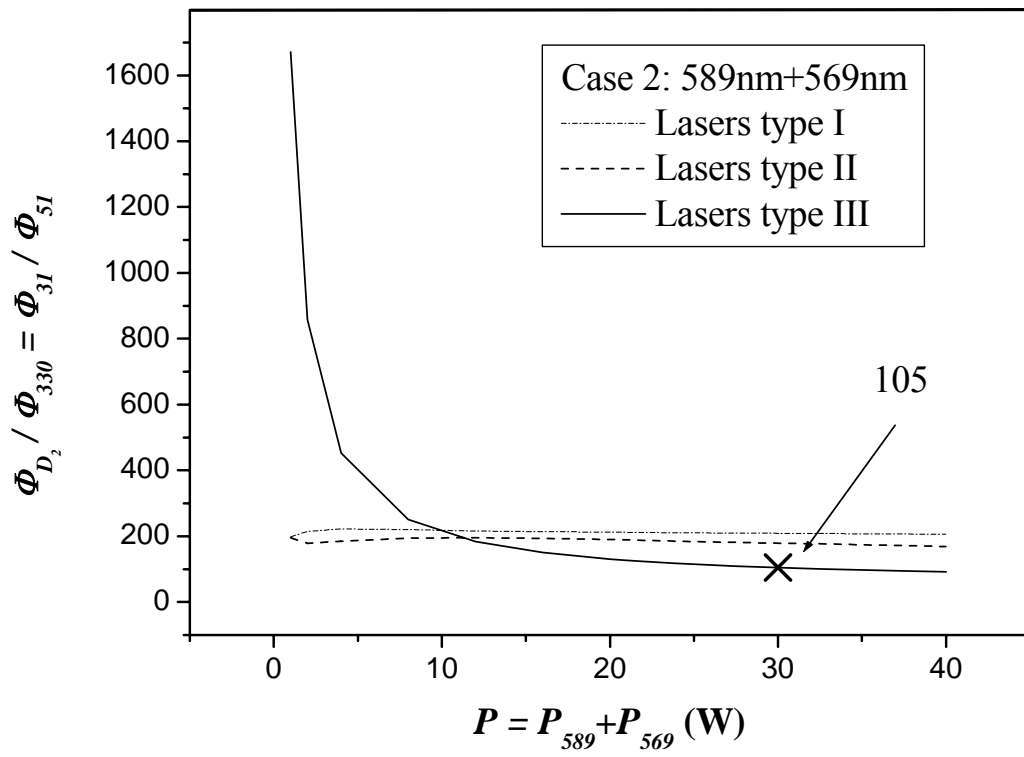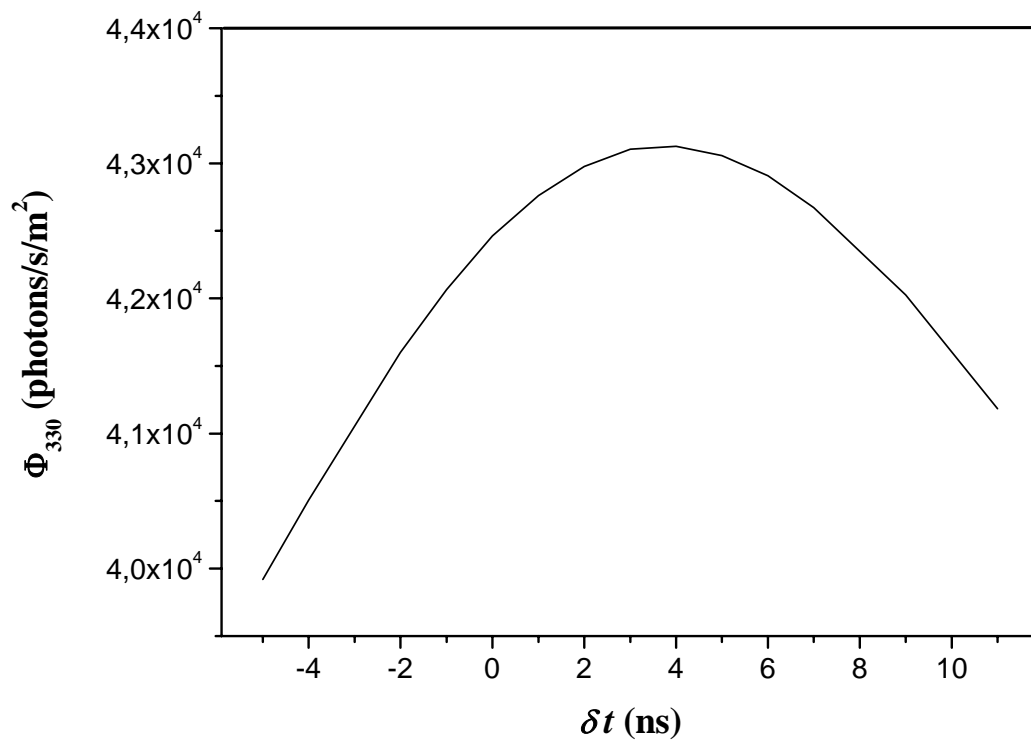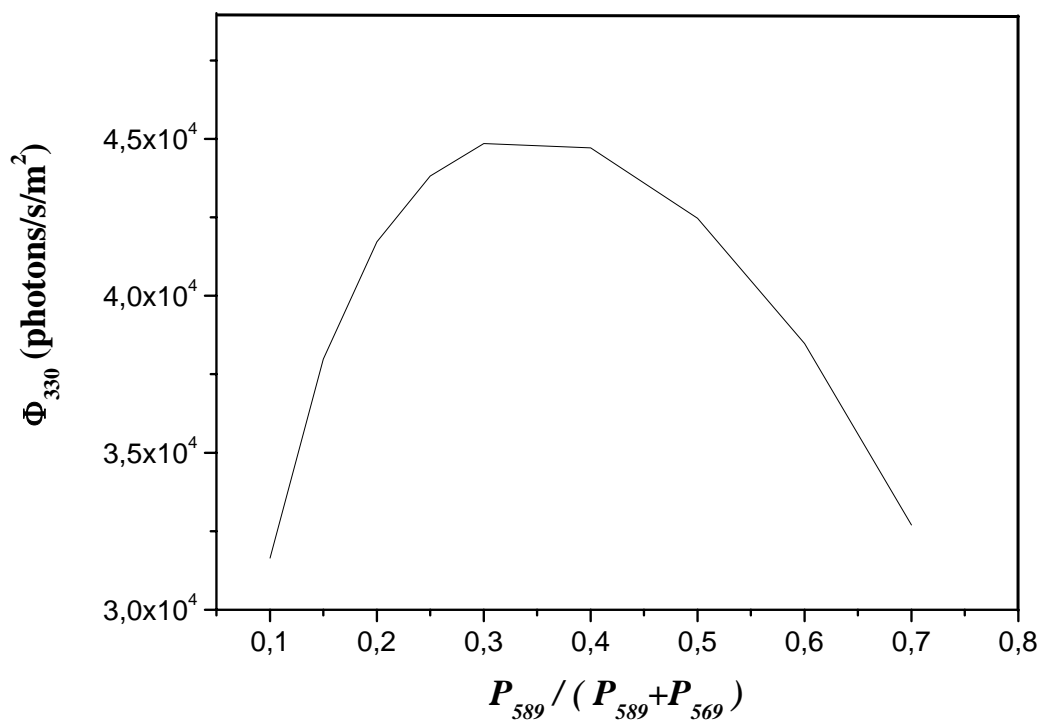
Figure 5

Figure 6

Figure 7

Figure 8

Figure 9

Figure 10

References

[1] A.R. Contos, P.L. Wizinowich, S. K. Hartman, D. Le Mignant, C.R. Neyman, P.J. Stomski and D. Summers, "Laser guide star adaptive optics at the Keck Observatory", Proceedings of Spie, **4839,** 370-380 (2003).

[2] D. Bonaccini, W. Hackenberg, M.J. Cullum, E. Brunetto, T. Ott, M. Quattri, E. Allaert, M. Dimmler, M. Tarenghi, A. Van Kersteren, C. Di Chirico, B. Buzzoni, P. Gray, R. Tamai, and M. Tapia, "ESO VLT laser guide star facility", in *Adaptive Optics Systems and Technology II*, Robert K. Tyson, Domenico Bonaccini, Michael C. Roggemann, eds., Proceeding of SPIE **4494**, 276-289 (2002).

[3] C. d'Orgeville, B.J. Bauman, J.W. Catone, B.L. Ellerbroek, D.T. Gavel, and R.A. Buchroeder, A. Richard, "Gemini north and south laser guide star systems requirements and preliminary designs", in *Adaptive Optics Systems and Technology II*, Robert K. Tyson, Domenico Bonaccini, Michael C. Roggemann, eds., Proceedings of SPIE **4494**, 302-316 (2002).

[4] J.Drummond, J.Telle, C.Denman, P.Hilman, and A.Tuffli, "Photometry of a sodium Laser Guide Star at Starfire Optical Range", Pub.of the Astron. S. of the Pacific **116**,278-289, (march 2004); J.M. Telle, P.W. Milonni, and R.Q. Fugate, " Update on 589-nm

sodium star pump laser requirements", in *Adaptive Optical Systems Technology*, Peter L. Wizinowich, ed., Proceeding of SPIE **4007**, 252-257 (2000).

[5] S.S. Olivier, C.E. Max, J. An, K. Avicola, H.D. Bissinger, J.M. Brase, H.W. Friedman, D.T. Gavel, B. Macintosh, and K.E. Waltjen , "First significant image improvement from the Lick Observatory laser guide star adaptative optics system", Am. Astro. Soc. **28**, 1324-1328 (1996).

[6] P. Wizinovich, D. Le Mignant, P. Stomski, D. Scott, Acton, A. Contos, C. Neyman, "Adaptive optics developments at Keck Observatory", Proceedings of SPIE **4839** (2003).

[7] I. S. McLean and S. Adkins, "Instrumentation at the Keck Observatory", Proceeding of SPIE **5492**, (2004).

[8] R. Foy and J.P. Pique, " Lasers in Astronomy ", Handbook of Laser Technology and Applications, Institute of Physics Publishing, edited by Colin E. Webb and Julian D.C. Jones, Volume I, 2581-2624 (Mar. 2004).

[9] R. Foy, private communication.

[10] R. Foy, A. Migus, F. Biraben, G. Grynberg, P.R. Mclluough, M. Tallon, "The polychromatic artificial sodium star: A new concept for correcting the atmospheric tilt", Astron. Astrophys.Suppl.Ser., **111**, 569-578(1995)

[11] J.P. Pique, S. Farinotti, An efficient modeless laser for a mesospheric sodium laser guide star", J. Opt. Soc. Am. B, **20**(10), 2093-2101(October 2003)

[12] M.Schöck, R.Foy, M.Tallon, L.Noethe, and J.P. Pique "Performance analysis of polychromatic laser guide stars used for wave front tilt sensing", Mon. Not. R. Astron. Soc. **337**, 910-920 (2002)

[13] C. d'Orgeville and F. Rigaut, private communication.

[14] M. van Dam, private communication.

[15] Vaillant J., Thiebaut E., Tallon M., "ELPOA: Data processing of chromatic differences of the tilt measured with a polychromatic laser guide star", Proceeding of SPIE, Vol. **4007**, Wizinowich P. L. (ed.), Adaptive Optical Systems Technology, p. 308 (2000).

[16] G. Mégie, F. Bos, J.E. Blamont and M.L. Chanin, "Simultaneous nighttime LIDAR measurements of atmospheric sodium and potassium", Planet. Space Sci., Vol. **26**, p. 27-35 (1978).

[17] K.H. Kwon, D.C. Senft, C.S. Gardner, "Lidar Observations of Sporadic Sodium Layers at Mauna Kea Observatory, Hawaii", J. Geophys. Research. **93,** 14199-14208 (november 1988).

[18] L. Michaille, J.B. Clifford, J.C. Dainty, T. Gregory, J.C. Quartel, F.C. Reavell, R.W. Wilson and N.J. Wooder, "Characterization of the mesospheric sodium layer at La Palma", Mon. Not. R. Astron. Soc. **328**, 993-1000 (2001).

[19] C.S. Gardner and J.D. Shelton, "Density response of neutral atmospheric layer to gravity wave perturbations", J. Geophys. Res. **90**, 1745-1754 (1985).

[20] C.W. Allen, Astrophysical Quantities , University of Lodon the Athlone Press, 25-26 (1973).

[21] M. Schöck, , J.P. Pique, A. Petit, P. Chevrou, V. Michau, G. Grynberg, A. Migus, N. Ageorges, V. Bellanger, F. Biraben, R. Deron, H. Fews, R. Foy , F. Foy, C. Högemann, M Laubscher, D. Müller, C. d'Orgeville, O. Peillet, M. Redfern, , P. Segonds, R. Soden,

M. Tallon, I. Tallon, E. Thiebaut, A. Tokovinin, J. Vaillant and J.M. Weulersse, "ELP-OA: measuring the wavefront tilt without a natural guide star", in *Propagation and Imaging through the Atmosphere IV*, M. C. Roggemann, ed, Proceeding of SPIE **4125**, 41-52 (2000).

[22] R. Foy, J.P. Pique, A. Petit, P. Chevrou, V. Michau, G. Grynberg, A. Migus, N. Ageorges, V. Bellanger, F. Biraben, R. Deron, H. Fews, F. Foy, C. Högemann, M Laubscher, D. Müller, C. d'Orgeville, O. Peillet, M. Redfern, M. Schöck, P. Segonds, R. Soden, M. Tallon, I. Tallon, E. Thiebaut, A. Tokovinin, J. Vaillant and J.M. Weulersse, « ELP-OA : Toward the tilt measurement from a polychromatique laser guide star », Proceeding of SPIE Meetings, Astronomical Telescopes and Instrumentation **4125**, 25-31 (March 2000).

[23] R. Foy, J.P. Pique, A. Petit, P. Chevrou, V. Michau, G. Grynberg, A. Migus, N. Ageorges, V. Bellanger, F. Biraben, R. Deron, H. Fews, F. Foy, C. Högemann, M Laubscher, D. Müller, C. d'Orgeville, O. Peillet, M. Redfern, M. Schöck, P. Segonds, R. Soden, M. Tallon, I. Tallon, E. Thiebaut, A. Tokovinin, J. Vaillant and J.M. Weulersse, « Polychromatic Guide Star : Feasibility study », SPIE Meetings, High Power Laser **4065**, 23-28 April 2000, Santa Fe, New Mexico.

[24] R. Foy, M. Tallon, I. Tallon-Bosc, E. Thiébaut, J. Vaillant, F.C. Foy, D. Robert, H. Friedman, F. Biraben, G. Grynberg, J.P. Gex, A. Mens, A. Migus, J.M. Weulerse and D.J. Butler, "Photometric observations of a polychromatic laser guide star", J. Opt. Soc. Am. **17**, 2236-2242 (2000).

[25] C.E. Max, K. Avicola, J.M. Brase, H.D. Bissinger, J. Duff, D.T. Gavel, J.A. Horton, R. Kiefer, J.R. Morris, S.S. Olivier, R.W. Presta, D.A. Rapp, J.T. Salmon, and K.E. Waltjen, "Design, layout, and early results of a feasibility experiment for sodium-layer laser-guide-star adaptive optics" , J. Opt. Soc. Am. A **11**(2), 813-824 (1994)

[26] C.A. Denman, P.D. Hillman, G.T. Moore, J.M. Telle, J.D. Drummond and A.L. Tuffli, "20W CW 589 nm sodium beacon excitation source for adaptive optical telescope applications", Optical Marerials **26**, 507-513 (2004).

[27] D.M. Pennington, J.W. Dawson, A. Drobsoff, Z. Liao, S. Payne, D. Bonaccini, W. Hackenberg and L. Taylor, « Compact fiber laser approach to 589 nm laser guide stars », CLEO **2**, 1 (2004).

[28] W. Hackenberg and D. Bonaccini, « Fiber Raman laser development for multiconjugate adaptive optics with sodium laser guide stars», Proceeding of SPIE **4494**, 271-275 (2002).

[29] K. Avicola, J.M. Brase, R.J. Morris, H. Bissinger, J.M. Duff, H.W. Friedman, D.T. Gavel, C.E. Max, S.S. Olivier, R. Presta, D.A. Rapp, J.T. Salmon, and K. Valtjen, "Sodium-layer laser-guide-star experimental results", J. Opt. Soc. Am. A **11**, 825-831 (1994).

[30] J. Biegert and J.C. Diels, « Feasability study to ceate a polychromatic guidestar in atomic sodium », Phys. Rev. A **67**, 043403 (2003).

[31] S. Fournier, "Quelques technologies laser récentes et leurs applications", Photonics, n°18, (june 2005) ; S. Venkat, « Laser developpement expand LDI capabilities », CircuiTree, (2005).

[32] Y. Louyer, F. Balembois, M.D. Plimmer, T. Badr, P. Georges, P. Juncar, and M.E. Himbert, « Effcient cw operation of diode-pumped Nd:YLF lasers at 1312.0 and 1322.6 nm for a silver atom optical clock », Optics Com., **217**, 357-362 (2003).